ingegneria sismica
International Journal of Earthquake Engineering
Anno XXXVI – Num.3

SEISMIC PERFORMANCE OF SUPERELASTIC TENSEGRITY BRACES

Filipe Santos[1], *Gianmario Benzoni*[2], *Fernando Fraternali*[3]

[1]CERIS and Department of Civil Engineering, Faculdade de Ciências e Tecnologia, Universidade Nova de Lisboa, Caparica, Portugal

[2]Department of Structural Engineering, University of California San Diego, CA, USA

[3]Department of Civil Engineering, University of Salerno, Fisciano (SA), Italy

SUMMARY: *This paper explores the capabilities of a superelastic, tensegrity-inspired bracing system acting as a seismic protection device. The metamaterial-type response of the proposed structure, which is related to its geometry more than to the nature of the employed materials, yields a passive control device with optimized structural response. It operates as a lightweight mechanical amplifier for longitudinal displacements. The enhanced energy dissipation and the re-centering capacity of the proposed tensegrity-SMA braces are demonstrated through experimental tests, and the seismic analysis of a benchmark structure. The effective performance of the proposed bracing in reducing the seismic damage of the served building paves the way to the design of novel seismic energy dissipation devices that combine tensegity and superelasticity concepts.*

KEYWORDS*: Seismic design, Bracing systems, Tensegrity structures, Shape-memory alloys, Energy dissipation, Recentering*

1 Introduction

In order to comply with the seismic performance required by modern structural codes, buildings are expected to provide adequate safety for design level earthquake excitations, with limited levels of structural and nonstructural damage. However, when subjected to strong ground motions, they mostly rely on their inherent ductility to prevent collapse, which is generally associated with a distributed inelastic response of the structural members and large permanent deformations. Repair costs and business downtime can make it financially unreasonable to repair a building after an earthquake [Dan, 2018]. Thus, innovative seismic structural protection systems, based in novel energy dissipation devices with self-centering capabilities, which minimize damage and substantially reduce repair costs following an earthquake, are currently needed [Longo *et al*., 2009, Giugliano *et al*., 2010, Menna *et al*., 2015, Chang and Araki, 2016, Montuori *et al*., 2016, Longo *et al*., 2016, Dell'Aglio *et al*., 2017, Piluso *et al*., 2019].

A number of studies have shown the great potential of tensegrity structures (TSs) when acting as impact protection and energy absorption devices [Skelton *et al*., 2010, Fraternali *et al*.,

Corresponding author: Fernando Fraternali, Department of Civil Engineering, University of Salerno, Italy.
Email: f.fraternali@unisa.it

2014, Rimoli, 2014]. Particularly interesting is the case of T-bar and D-bar tensegrity systems, which have been optimally designed in [Skelton *et al*., 2010, Montuori and Skelton, 2017, Goyal *et al*., 2019] in order to achieve large buckling load to mass ratios, and very high energy storage capacity with minimal mass. Generally, TSs are arranged in very stable and efficient geometrical configurations, that can achieve great strength with small mass, since the material is only used in the essential load paths. TSs are easy to fold, deploy and adjust, offering many operational and portability advantages [Skelton and Oliveira, 2010, Skelton *et al*., 2002]. As their members simply respond only in tension and/or compression and are not subjected to bending or torsion, such systems can be accurately modeled from the mechanical point of view. It is also worth noting that the mechanical response of TSs mainly originates from their geometry, which implies that they are applicable from small to large scales, with physical limitations only depending on the nature of the employed materials [Juan and Tur, 2008, Sultan *et al*., 2002]. Their use is seismic engineering calls for special attention, since TSs are able to combine enhanced stiffness, strength and/or energy dissipation capacity with lightweight design.

This paper develops and investigates a seismic force resisting bracing system with tensegrity architecture, which efficiently limits inter-story drifts while dissipating energy. The proposed brace is based on a D-bar TS that features four compressive struts forming a rhomboidal structure and two perpendicualr tension ties attached to the extremities of the struts. In order to provide the proposed tensegrity bracing with increased damping and re-centering capabilities, the energy dissipation device proposed in the present work makes use of superelastic tendons built up of NiTi shape-memory alloy wires. These binary metallic alloys can develop martensitic transformations, which are solid state crystallographic transformations between a high energy phase, austenite, and a low energy phase, martensite. The austenite-martensite transformations can be triggered either by temperature or stress and enable Shape Memory Alloy (SMA) elements to develop a wide hysteresis, while subjected to mechanical cycles comprising strains up to 8%, with no residual deformations [Menna *et al.*, 2015]. This superelastic hysteresis translates into the ability of SMAs to dissipate energy and has made them particularly suited for kernel elements in seismic mitigation bracing systems [Menna *et al.*, 2015, Chang and Araki, 2016, Asgarian and Moradi, 2011, Miller *et al.*, 2012, Yang *et al.*, 2010].

The paper is organized as follows. Section 2 presents the basic features of superelastic tensegrity braces, as well as the geometrical advantages associated with such structural elements. Section 3 illustrates an experimental analysis of a small scale tensegrity brace, which is used to validate a numerical model of the bracing system. The assessment of the structural damage of a three-story building is presented in Sect. 4, on using the HAZUS methodology to define structural damage states [HAZUS-MH, 2003]. The main conclusions of the present study and directions for future work are presented in Section 5.

2 D-bar bracing device

In the original definition of tensegrity structures, the compressive members forming such elements are disconnected each other, yielding the so-called Class 1 tensegrity systems [Skelton *et al*., 2002, Fraternali *et al.*, 2014]. This definition has been generalized by Skelton and de Oliveira in [Skelton and Oliveira, 2010], by introducing the notion of Class k tensegrity systems, which show a maximum of k members attached to the same node of the structure.

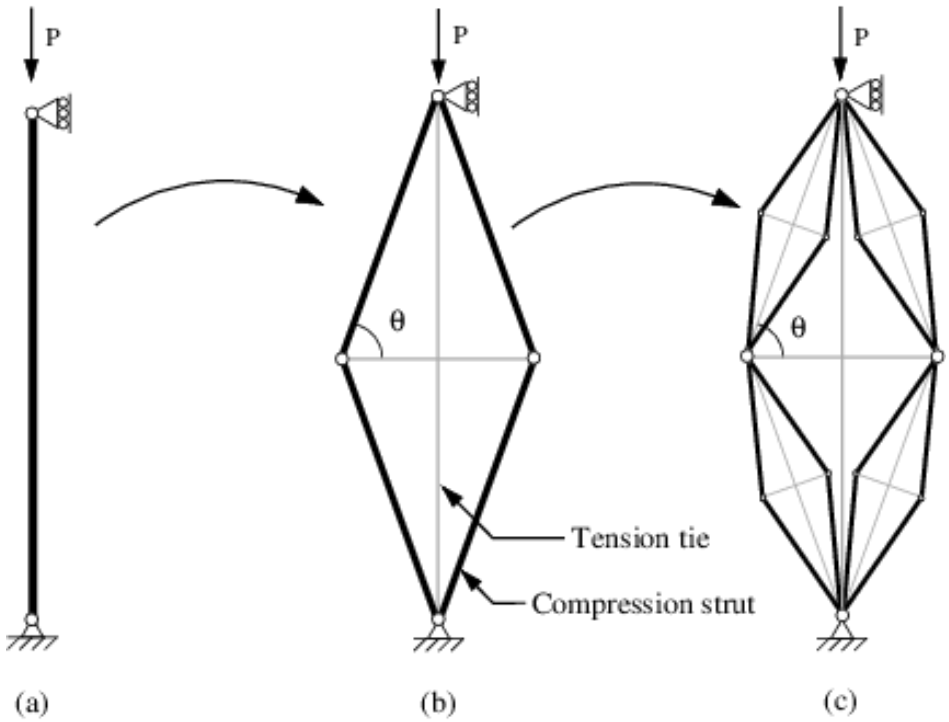

Figure 1: *Proposed C4T2 tensegrity brace*

In order to design an efficient bracing system, which is able to carry compressive loads with small mass, we here employ a Class 2 tensegrity system comprising four compressive struts and two tendons (C4T2). The proposed device exhibits the geometry represented in Figure 1(b). It is worth noting that the geometry of the C4T2 brace resembles that of the scissor-jack damper studied in [Șigaher and Constantinouu, 2003], with the difference that the C4T2 brace includes a longitudinal SMA cable, which is absent in the scissor-jack damper, and replaces the damper of such a system with a transverse SMA cable. The basic principle responsible for the compression efficiency of this brace is associated with a first geometrical advantage, which derives from the use of tensile members exhibiting large load to mass ratios. It is worth mentioning the fractal design approach proposed in Skelton and de Oliveira [Skelton and Oliveira, 2010], which leads to subdivide the basic D-bar unit shown in Figure 1(b) through an iterative algorithm that replaces each strut with a smaller scale D-bar system. The first iteration of such a a self-similar subdivision procedure leads to the structure illustrated in Figure 1(c), which is out of the scope of the present study.

Let us now design the C4T2 brace in Fig. 1(b) so as it exhibits the same buckling load P of the straight column represented in Figure 1(a), whose mass is hereafter denoted with the symbol m_0. Assuming zero initial self-stress in the C4T2 brace, and supposing that the vertical tendon goes slack under compression loading (no compression response), it is easy to show that the above design procedure leads to a total mass m_1 of the C4T2 system given by the following formula: $m_1 = m_0 (2 \sin^5\theta)^{-\frac{1}{2}}$ [Skelton and Oliveira, 2010]. This formula is graphically illustrated by the graph in Figure 2, where the mass ratio m_0/m_1 is plotted as a function of the angle θ. The results in Figure 2 highlight that m_1 is lower than m_0 for aspect angles θ of the C4T2 bracing (Figure 1(b)) greater than 60.5 degrees, with a mass reduction m_1/m_0 about equal to 26% for θ = 80 degrees.

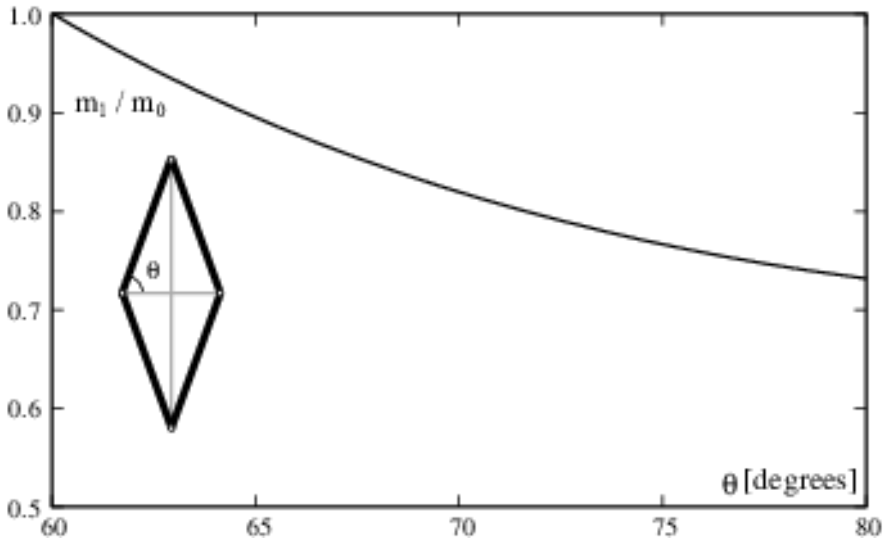

Figure 2: *Mass ratio m_1/m_0 as a function of the angle θ.*

The amount of damping that can be delivered by passive bracing systems during dynamic events is related to the level of displacements experienced by the braces [Mathias *et al.*, 2016].

Generally, increased displacements lead to higher damping. However, the relative displacements between the extremities of structural braces, even during seismic events, can be relatively low (refer, e.g., to [Barbagallo *et al.*, 2019, Chou *et al.*, 2019] and references therein). This hinders the performance of SMA based bracing systems, which rely on high deformations to dissipate energy.One interesting feature of the proposed C4T2 tensegrity brace is that it acts as a mechanical amplifier of the longitudinal displacements along the transverse direction, increasing the level of deformations experienced by the transverse SMA tendons, and, hence, potentiating damping.

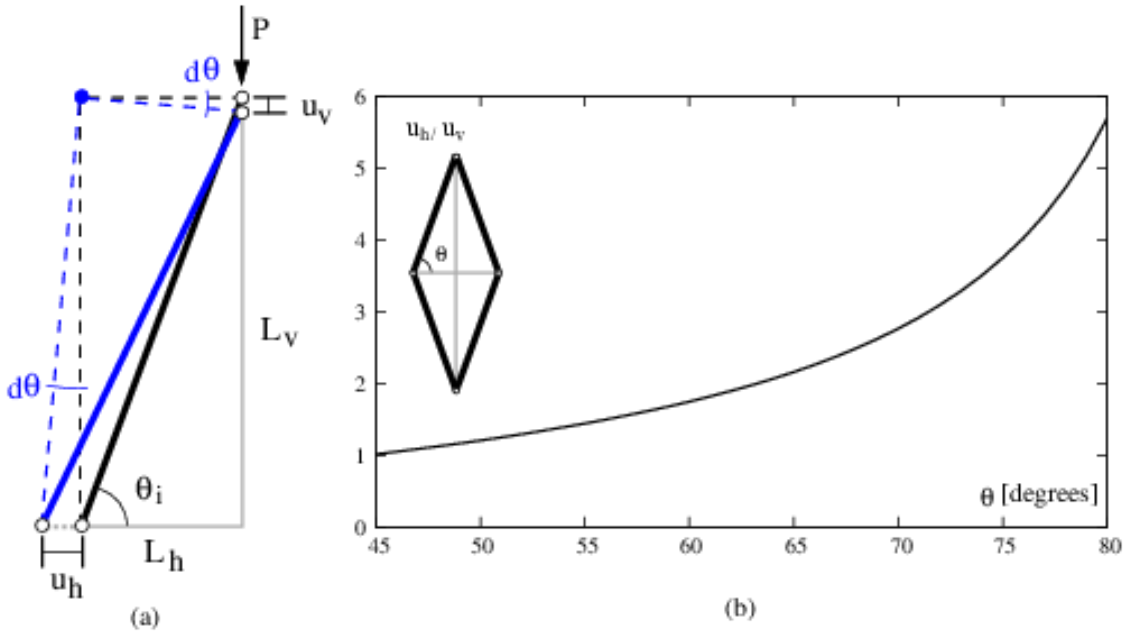

Figure 3: *Displacement amplification factor of the C4T2 brace in the small displacement regime.*

This second geometrical advantage of the proposed device is illustrated in Figure 3(a), where it can be seen that the longitudinal displacement u_v (positive if directed downward), associated with load P, is transformed into a higher transverse displacement u_h (positive if produces the extension of the transverse string).
On assuming that the bars of the structure behaves as rigid bodies during an arbitrary transformation of the structure [Skelton and Oliveira, 2010], the following kinematic compatibility holds: $L^2 = (\frac{L_v}{2} - \frac{u_v}{2})^2 - (\frac{L_h}{2} + \frac{u_2}{2})^2 = const.$ In the small displacement regime, it is easy to show that such a relationship yields: $\frac{u_h}{u_v} = \frac{L_v}{L_h} = \tan\theta$ (Figure 3). The u_h/u_v amplification factor therefore tends to infinity as the angle θ tends to 90 degrees, under the assumption of infinitesimal strains, and one notes that it results $u_h/u_v = 1.73$ for $\theta = 60$ degrees, and $u_h/u_v = 5.67$ for $\theta = 80$ degrees.

3 Experimental and numerical characterization of the constitutive response of a C4T2 brace

A small scale physical model of a C4T2 brace was built in order to experimentally study the influence of the internal angle θ on the mechanical response of the proposed device. Each of the compressive struts was made out of two parallel 440 mm long pine wood bars, with 35 × 5 mm ^{2} cross sections, connected between themselves at the mid-length of the bars. Hinges were placed at the extremities of the struts in order to allow for free rotation. NiTi superelastic wires (d = 0.406 mm), obtained in as drawn state from Euroflex GmbH, were used to form the tendons of the system, with a composition of 54.5-57 wt.-% Ni. The geometry of the C4T2 brace was defined with an internal angle θ of 60 degrees, as reported in Table 1. The system is under zero initial self-stress in the freestanding configuration.

Table 1: Tested configuration for the C4T2 brace.

θ	L	L $_h$	L $_v$
(degrees)	(mm)	(mm)	(mm)
	440	440	762

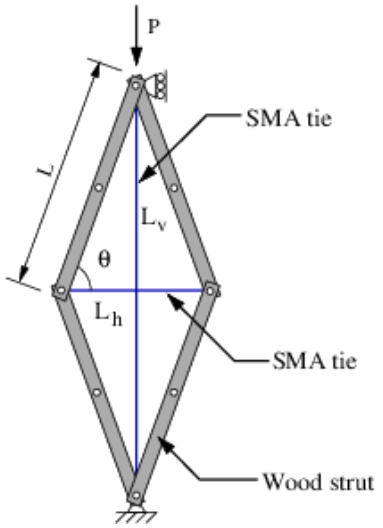

Prior to applying uniaxial cyclic testing to the C4T2 brace, a similar tensile test was performed on a NiTi wire sample, using a Zwick/Roell Z050 electro-mechanical testing machine operating in strain control. Such a test was performed at an ambient temperature of

20 °C, with a strain-rate of approximately 0.12%/s, comprising seven cycles of increasing strain amplitude (from 1 % up to 7 % axial strain). The wire was previously preconditioned by 20 loading-unloading tensile cycles in order to stabilize the superelastic behavior, since NiTi SMAs are known to be prone to cyclic instability [Casciati and Marzi, 2010, Carreras *et al.*, 2011].

The cyclic testing of the brace was next performed under axial displacement control, up to a maximum displacement of 10 mm, with a displacement-rate of approximately 1 mm/s. It can be easily demonstrated that the axial displacement (u_L) of a diagonal brace can be computed as a function of the corresponding inter-story drift ratio (δ), using the expression $\delta = u_L / (L \sin\alpha \cos\alpha)$, with L being the length of the brace, and α being the angle that this element forms with its horizontal projection. If we consider α = 30 degrees, a longitudinal displacement of 10 mm corresponds to an inter-story drift ratio of 2.6%. Figures 4(a),(b) show images of the NiTi wire and the C4T2 brace under testing, respectively. The experimental stress-strain response of the NiTi wire sample to seven consecutive tensile cycles is shown in Figure 5.

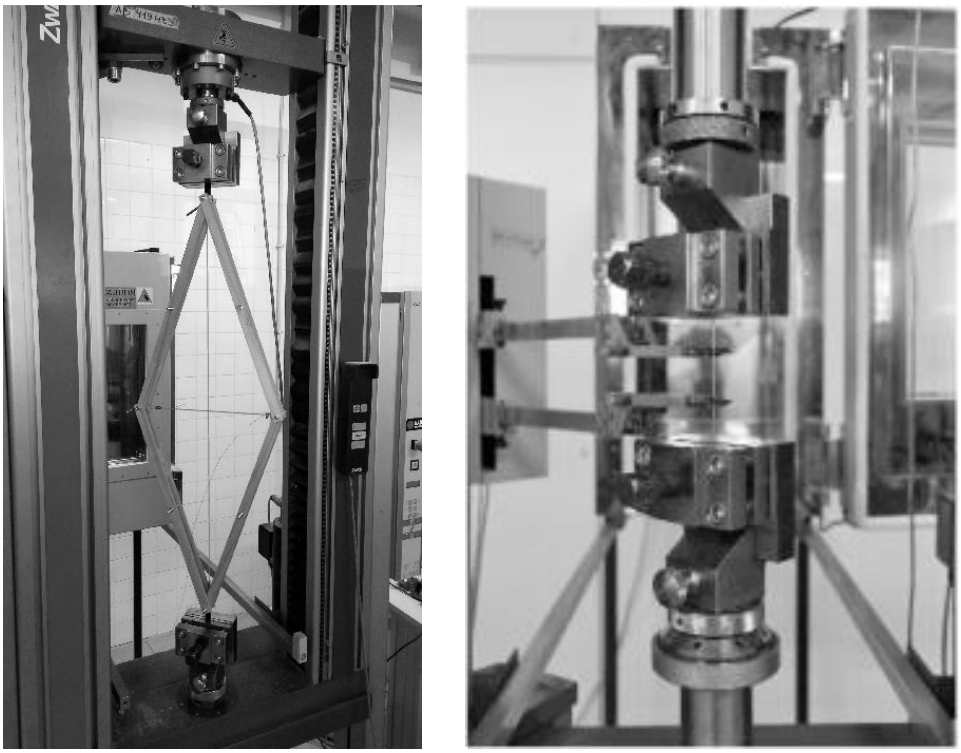

(a) NiTi wire (b) C4T2 brace

Figure 4: Samples under tensile testing.

A numerical analysis of the brace response under loading was also performed, aiming to simulate its mechanical behavior during the experimental tensile tests, and in order to to obtain a validated C4T2 numerical model. Such a study was conducted through the commercial nonlinear finite element (FE) code SeismoStruct [SeismoStruct, 2019], which incorporates the simplified uniaxial model for SMAs developed by Fugazza [Fugazza, 2003], based on the constitutive model proposed by Auricchio and Sacco [Auricchio and Sacco,

1997]. In spite of its simplicity, this temperature and rate-independent model can be effectively used to simulate the response of SMAs for seismic applications without significant loss of accuracy [Amarante dos Santos and Cismaşiu, 2010]. The key parameters used to express the complete stress-strain relation of the SMA ties are presented in Table 2. Their calibration was performed through the fitting of the experimental stress-strain response shown in Figure 5. Gap_hook link elements were used to prevent the cables from working in compression.

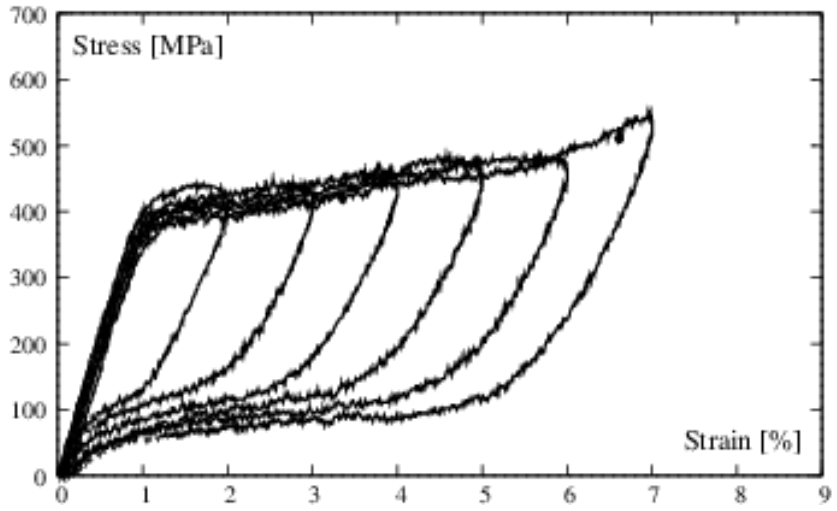

Figure 5: Stress-strain response of the NiTi wire sample to 7 consecutive tensile cycles.

Table 2: Constitutive parameters of the adopted SMA model.

Parameters	Unit	Value
Elastic modulus	GPa	40
Austenite to martensite starting stress	MPa	350
Austenite to martensite finishing stress	MPa	500
Martensite to austenite starting stress	MPa	200
Martensite to austenite finishing stress	MPa	100
Yield strain limit	%	1
Recoverable pseudoelastic strain limit	%	7

The numerical and experimental results for the vertical force F_v vs. vertical displacement u_v response of the C4T2 brace are presented in Figure 6, on assuming downward directed displacements and forces as positive. One observes the formation of the typical flag-shaped hysteresis loops in the F_v - u_v response, with the total recovery of the imposed displacements after unloading. Under the previously mentioned assumption of zero initial pretension of the SMA wires, it is worth noting that the response of the C4T2 brace is such that the vertical string is slack and the horizontal string is tensioned under positive (i.e., downward pointing) forces, while, oppositely, the vertical string is tensioned and the horizontal string is slack under negative (upward pointing) forces. The results in Figure 6 highlight the noticeable transverse displacement amplification ability of the C4T2 brace, which allows the system to absorb remarkably high values of positive vertical forces, due to the ability of the horizontal wire to exploit high austenite-martensite transformation ratios.

The response to negative vertical forces is instead not affected by such a geometric amplification effect (since the horizontal string are slack), and one indeed observes that the C4T2 brace is able to absorb lower vertical forces in such a regime, as compared to the response under positive vertical loads. The effective viscous damping of the tested C4T2 brace, computed as described in [30] in the displacement range $u_h \in [-10,10]$ mm, is approximatively equal to 12%. We observe an overall good matching between numerical and experimental results in Figure 6, which confirms that the adopted numerical model reasonably captures the main features of the experimental force-displacement response of the C4T2 brace.

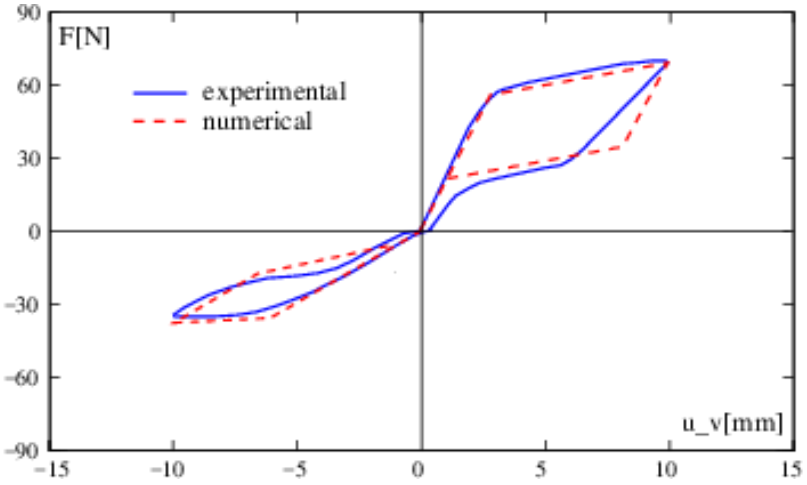

Figure 6*:* Comparison between numerical and experimental force-displacement diagrams.

4 Seismic analysis of a benchmark building

The present section studies the seismic behavior of a three-story benchmark steel building, which is equipped with C4T2 braces featuring an aspect angle θ equal to 70 degrees (C4T2 model). For the sake of comparison, we also analyze the seismic response of the unbraced building (WB model) and, finally, the responses of the building reinforced with simple bracing systems, which use either Steel or SMA cables as braces (Steel and SMA models, respectively).

4.1 General description of the building

A three-story (3-story) steel building is considered [Ohtori *et al*., 2004], which was designed for the SAC project of the US Federal Emergency Management Agency (FEMA) [SAC, 1994]. The dimensions of the examined building are as follows: 36.58 m by 54.87 m in plan, and 11.89 m in elevation. The bays are 9.15 m wide, in both directions, with four bays in the north-south (N-S) direction and six bays in the east-west (E-W) direction. The lateral load-resisting system of the building is comprised of steel perimeter moment-resisting frames (MRFs) with simple framing between the two furthest south E-W frames. The interior bays of the structure contain simple framing with composite floors. The columns are 345 MPa steel. The columns of the MRF are wide-flange. The levels of the 3-story building are numbered with respect to the ground level (see Figure 7). The 3rd level is the roof. Typical floor-to-

floor heights are 3.96 m. The column bases are modeled as fixed (at the ground level) to the ground. The floors are composite construction comprising 248 MPa steel wide-flange beams acting compositely with the floor slab. The floor system provides diaphragm action and is assumed to be rigid in the horizontal plane. The inertial effects of each level are assumed to be carried evenly by the floor diaphragm to each perimeter MRF, hence each frame resists one half of the seismic mass associated with the entire structure. The 3-story N-S MRF is depicted in Figure 7. We refer the reader to Table 3 for the illustration of the steel wide flange profiles used for the columns and beams of the building under examination (according to ASTM A36 [ASTM A36, 1986]). An in-depth illustration of this building can be found in Ref. [Ohtori *et al*., 2004].

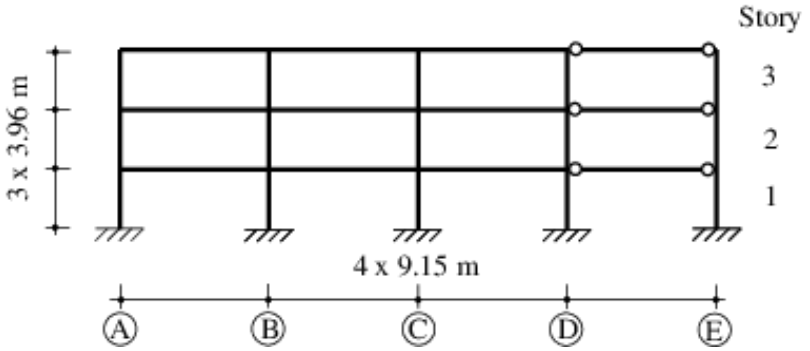

Figure 7: 3-Story N-S MRF of the examined building [25].

Table 3: Steel wide flange profiles used for the columns (Col.) and the beams of the examined building according to ASTM A36. Legend: MRC - moment resisting connection; HC - hinged connection; WA - weak axis.

Story	Col. A&D	Col. B&C	Col. E	Beams (MRC)	Beams (HC)
	W14x257	W14x311	W14x311 (WA)	W24 x 68	W21 x 44
	W14x257	W14x311	W14x311 (WA)	W30 x 116	W21 x 44
	W14x257	W14x311	W14x311 (WA)	W33 x 118	W21 x 44

4.2 Ground motions for the structural analysis

In order to evaluate proposed control strategies, two far-field and two near-field historical records were selected, giving a total of four historical ground acceleration records, which are hereafter briefly described. (i) El Centro. The N-S component recorded at the Imperial Valley Irrigation District substation in El Centro, California, during the Imperial Valley, California earthquake of May 18, 1940. (ii) Hachinohe. The N-S component recorded at Hachinohe City during the Tokachi-oki earthquake of May 16, 1968. (iii) Northridge. The N-S component recorded at Sylmar County Hospital parking lot in Sylmar, California, during the Northridge, California earthquake of January 17, 1994. (iv) Kobe. The N-S component recorded at the Kobe Japanese Meteorological Agency station during the Hyogo-ken Nanbu earthquake of January 17, 1995. The absolute peak accelerations of the earthquake records are 3.42, 2.25, 8.27, and 8.18 ms $^{-2}$, respectively. We consider different levels of scaling of such earthquake records, which include: 0.5, 1.0 and 1.5 scaling factors in the case of the El Centro and Hachinohe records; and 0.5 and 1.0 scaling factors in the case of the Northridge and Kobe records. This gives a total of ten earthquake records employed for the evaluation of the seismic performance of the examined building.

4.3 Seismic vulnerability assessment

The seismic vulnerability assessment of the building was performed in terms of peak and residual inter-story drift ratios under the ground motions described in the previous section. The seismic simulations were performed using the SeismoStruct code, which is able to accurately predict the distribution of damage both along the element span and across its cross-section depth [SeismoStruct, 2019]. The cross section of the SMA tendons in the C4T2 model was set to 19.25 cm^2 in order to allow for the development of the full extent of the martensitic transformation, under the heaviest seismic loading scenarios. For what concerns the SMA model, we again set the cross-section of the SMA cables to 19.25 cm^2, while in the Steel model we make use of steel cables with cross-section area of 7.70 cm^2, so as to balance the axial stiffness constants of SMA wires and steel cables. All the examined braces were arranged in a chevron configuration, as shown in Figure 8. In order to provide a safe assessment of the structural performance of the building, 5% Rayleigh damping was considered [Yang *et al*., 2010].

Figure 9 shows the force-displacement responses of the most stressed braces of the examined building models in correspondence with the heavier ground motions records, namely the Northridge and Kobe records, for different scaling factors.

The comparative analysis shown in Figure 9 highlights that the adoption of the C4T2 tensegrity bracing system (Fig. 8(a)) leads to a double-flag shaped superelastic hysteretic response of the braces, contrary to the Steel and SMA bracing models (Fig. 8(b)). The SMA braces indeed exhibit a single flag-type hysteretic response, which is active only when such element work in tension, since they do not react in compression. The Steel braces instead exhibit a plastic response when working in tension, and again zero response in compression. Due to the previously noted geometrical advantage of the C4T2 bracing, the adoption of such a strengthening technique makes it easier to reach the full extent of the martensitic transformation in the SMA wires, leading to higher dissipating capabilities of the structure. The energy dissipation capacity of the C4T2-braced building does not compromise the re-centering ability of the braces, which is instead not guaranteed in the steel-braced building, due to the irreversible plastic deformation of the steel cables.

Figure 10 illustrates the distributions along the height of the building of the peak inter-story drifts (Peak ISD) and residual inter-story drifts (Res. ISD), expressed as fractions of the inter-story height, under the scaled Northridge and Kobe ground motions. Fig. 11 instead provides bar diagrams of the average values of Peak ISD and Res. ISD along the height of the building, which were computed for all the ground motions described in the previous section.

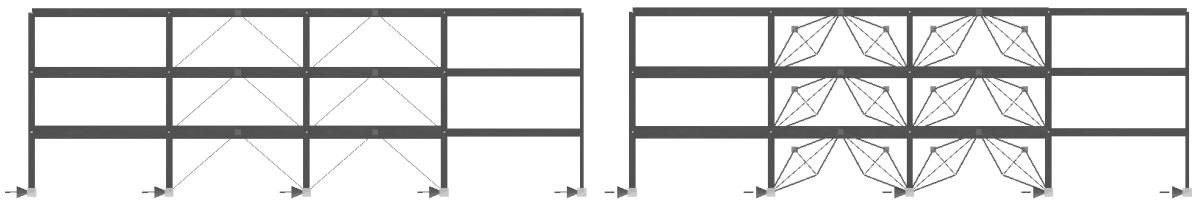

(a) Steel and SMA bracings (b) C4T2 bracing

Figure 8*:* 3-Story Benchmark Building with chevron bracings.

The assessment of the structural damage was performed using the HAZUS definition of average inter-story drift ratio of structural damage states [Mouroux and Brun, 2006, HAZUS-MH, 2003]. We refer to damage states that are associated with low-rise buildings and a Moderate-Code design level, which are divided into the following four categories: slight (0.6%), moderate (1.0%), extensive (2.4%) and collapse (6%).

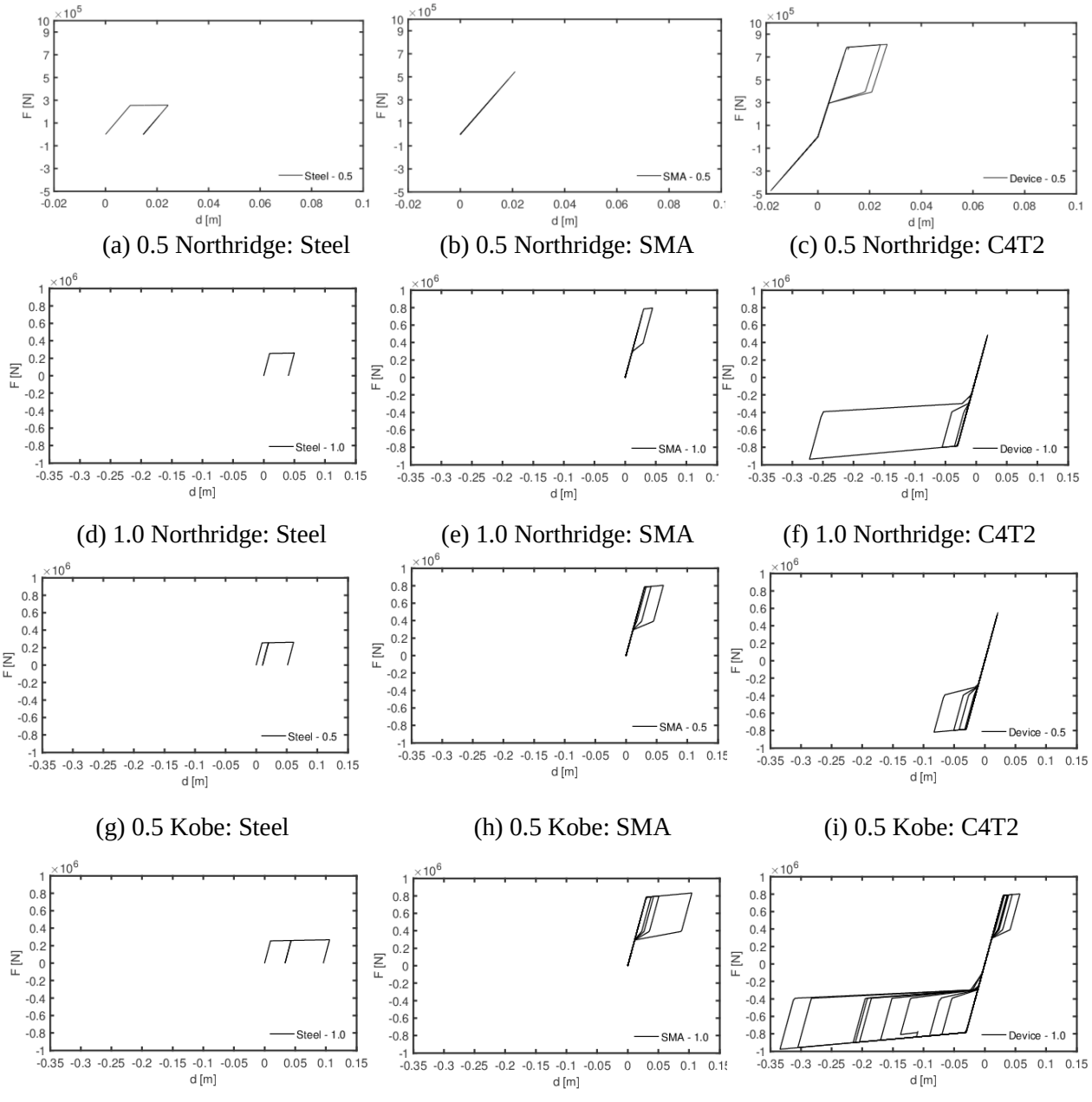

(a) 0.5 Northridge: Steel (b) 0.5 Northridge: SMA (c) 0.5 Northridge: C4T2

(d) 1.0 Northridge: Steel (e) 1.0 Northridge: SMA (f) 1.0 Northridge: C4T2

(g) 0.5 Kobe: Steel (h) 0.5 Kobe: SMA (i) 0.5 Kobe: C4T2

(j) 1.0 Kobe: Steel (k) 1.0 Kobe: SMA (l) 1.0 Kobe: C4T2

Figure 9: Force-displacement responses of the most stressed braces of the analyzed building models.

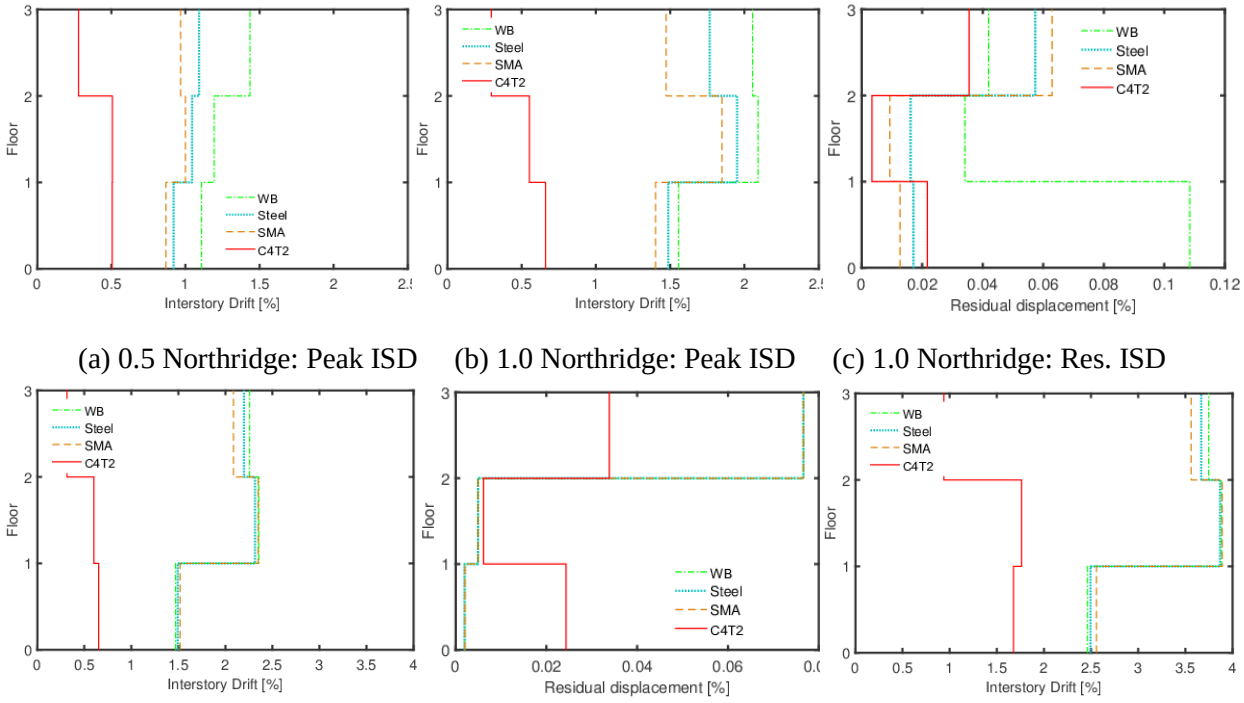

(a) 0.5 Northridge: Peak ISD (b) 1.0 Northridge: Peak ISD (c) 1.0 Northridge: Res. ISD

(d) 0.5 Kobe: Peak ISD (e) 1.0 Kobe: Peak ISD (f) 1.0 Kobe: Res. ISD

Figure 10*:* Peak and residual ISD along the height of the building.

The results in Figs. 10, Fig. 11 confirm that the the proposed C4T2 bracing shows a rather good seismic performance, especially under the heaviest ground motions analyzed in the present study, substantially reducing both the peak and residual ISD ratios exhibited by the building during the earthquake.

The maximum ISD ratio reduction is obtained for the 0.5 Kobe record, where the C4T2 bracing is able to decrease the damage state from extensive to slight. Overall, the C4T2-braced building shows the lowest values of Peak and Residual ISD ratios among all the building models examined in the present study, with exception of only two cases (over the 10 examined), which are related to the Hachinohe record, namely the Peak ISD for the 1.5 Hachinohe record and the Res. ISD for the 1.0 Hachinohe record. (cf. Fig. 11). We remark, however, that the SMA-braced building model is not able to exhibit a double-flag shaped superelastic hysteretic response, as we have already observed (Fig. 10).

The maximum values of the Peak ISD and Res. ISD of the C4T2-braced building, among all the examined earthquake records, are respectively equal slightly greater that 1.5% for Kobe 1.0, (approximatively equal to 1.5% for El Centro 1.5 and Hachinohe 1.5) and approximatively equal to 0.06 % (Hachinohe 1.5). With reference to the unaltered ground motion records and the CT42-braced building (scaling factor equal to 1.0), we observe a slight damage level in correspondence with the Northridge and Hachinohe records; a nearly moderate damage under the El Centro record; and a damage level comprised in between moderate and extensive in correspondence of the Kobe record. In the same conditions, the damage levels of the unbraced building are markedly extensive under the Kobe record, nearly extensive under the Northridge record, and comprised in between moderate and extensive under the El Centro and Hachinohe records.

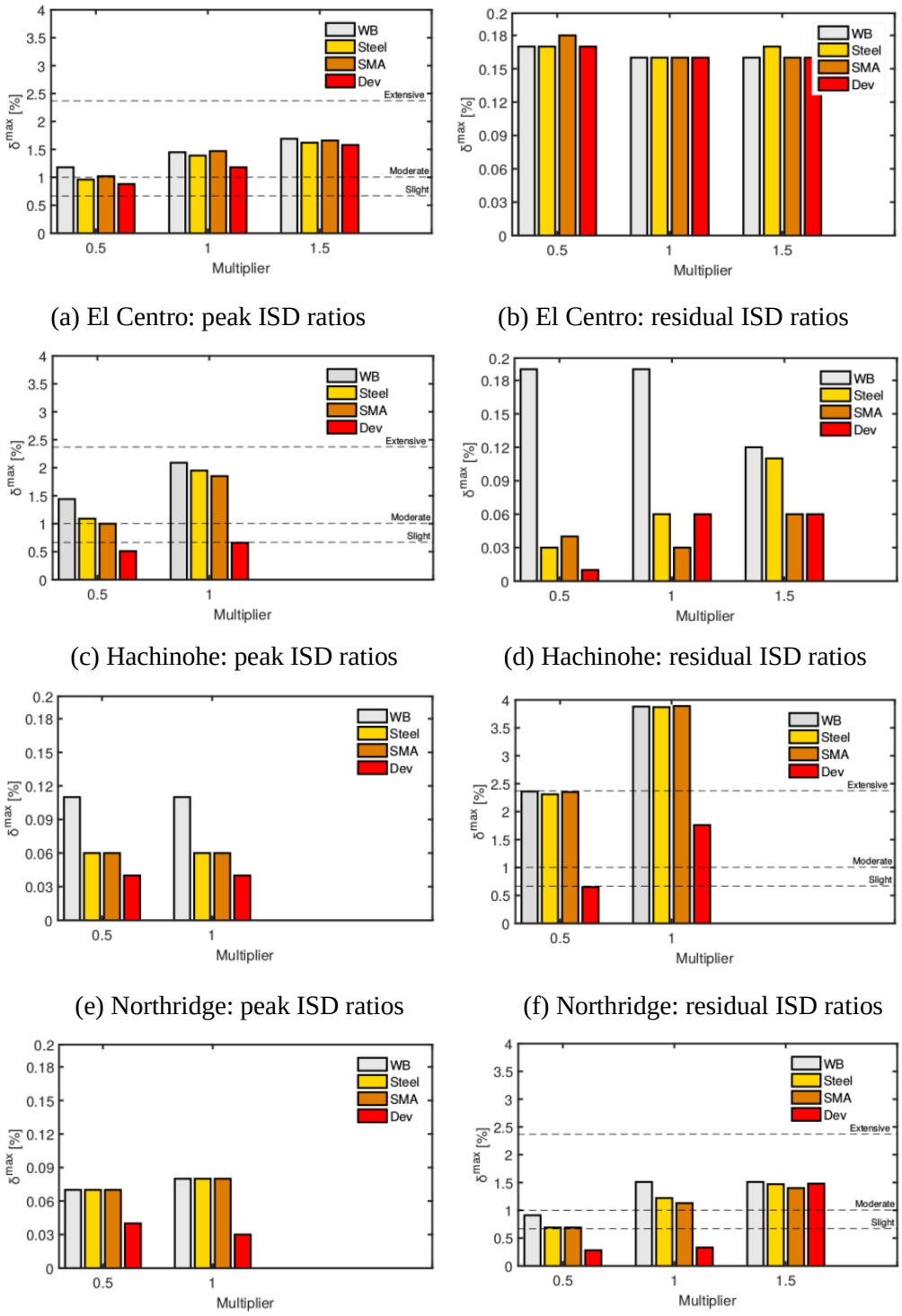

(a) El Centro: peak ISD ratios

(b) El Centro: residual ISD ratios

(c) Hachinohe: peak ISD ratios

(d) Hachinohe: residual ISD ratios

(e) Northridge: peak ISD ratios

(f) Northridge: residual ISD ratios

(g) Kobe: peak ISD ratios

(h) Kobe: residual ISD ratios

Figure 11: Bar diagrams of the average values of Peak ISD and Res. ISD along the height of the building for all the examined ground motions (Dev here indicates the C4T2 bracing system).

5 Conclusions

This study has analyzed the seismic response of tensegrity braces equipped with superelastic tendons. The given experimental and numerical results have shown hat such a bracing system can excel in structural seismic control. The main conclusions that can be drawn from the study presented in Sects. 2-4 are the following:

1. The compression efficiency of the C4T2 braces is ensured by the use of a tensegrity architecture (D-bar system) that exhibits large buckling load to mass ratios (cf. Sect. 2).

2. The C4T2 brace acts as a mechanical amplifier for longitudinal displacements, increasing the level of deformations experienced by the transverse SMA tendons, and, hence, potentiating the effective damping offered by the device (Sect. 2).

3. In spite of its simplicity, the adopted numerical model proved able to capture main features of the force-displacement response exhibited by the C4T2 brace (Sect. 3).

4. Based on the seismic vulnerability analysis presented in Sect. 4, it is possible to conclude that the C4T2 bracing system is able to successfully mitigate the earthquake induced damage, by markedly reducing the damage levels and the probability of collapse of the served building.

Future directions of the present work will be aimed at examining a large variety of configurations of the C4T2 bracing system, for different aspect angles θ, and self-similar subdivisions of the basic C4T2 module (cf., e.g., Figure 1(c)). Such a study will focus on the optimization of the transverse displacement amplification offered by such a device, and the symmetrization of the double-flag hysteretic response under cyclic loading, by playing with the geometry of the system, members' size and the initial pretension of the SMA tendons. The preparation of physical models will profit from additive manufacturing techniques employing both polymeric and metallic materials [Amendola *et al.*, 2015]. Additional future research lines will regard the design and experimental testing of chains and multilayered arrangements of D-bar units [Amendola *et al.*, 2017, Frateernali *et al.*, 2018], to be used as novel bracing systems of seismic resistant buildings, and next-generation dissipative springs with re-centering capabilities.

Acknowledgements

The authors would like to thank Tiago Ricardo who worked on the subject covered by the present study during his MS Thesis work at the Universidade Nova de Lisboa, providing precious assistance with the numerical simulations presented in Sects. 3 and 4. FF gratefully acknowledges financial support from the Italian Ministry of Education, University and Research (MIUR) under the 'Departments of Excellence' grant L.232/2016.

References

Amarante dos Santos, F. P., C. Cismaşiu, Comparison Between Two SMA Constitutive Models for Seismic Applications, Journal of Vibration and Control 16 (6) (2010) 897–914.

Amendola, A. C.J. Smith, R. Goodall, A. Auricchio, L. Feo, G. Benzoni, F. Fraternali, Experimental

response of additively manufactured metallic pentamode materials confined between stiffening plates. Composite Structures, 142 (2016), 254-262.

Amendola, A., E. Hernandez-Nava, R. Goodall, I. Todd, R.E. Skelton, F. Fraternali, On the additive manufacturing, post-tensioning and testing of bi-material tensegrity structures, Composite Structures, 131 (2015), 66–71.

Amendola, A., G. Benzoni, F. Fraternali, Non-linear elastic response of layered structures, alternating pentamode lattices and confinement plates, Composites Part B: Engineering, 115 (2017), 117-123.

Asgarian, B., S. Moradi, Seismic response of steel braced frames with shape memory alloy braces, Journal of Constructional Steel Research 67 (1) (2011) 65 – 74.

Auricchio, F., E. Sacco, A superelastic shape-memory-alloy beam model, Journal of Intelligent Material Systems and Structures 8 (6) (1997) 489–501.

Barbagallo, F., M. Bosco, E.M. Marino, P.P. Rossi, Seismic design and performance of dual structures with BRBs and semi-rigid connections. Journal of Constructional Steel Research, 158 (2019), 306-316.

Carreras, G., F. Casciati, S. Casciati, A. Isalgue, A. Marzi, V. Torra, Fatigue laboratory tests toward the design of SMA portico-braces, Smart Structures and Systems 7 (1) (2011) 41–57.

Casciati, S., A. Marzi, Experimental studies on the fatigue life of shape memory alloy bars, Smart Structures and Systems 6 (1) (2010) 73–85.

Chang, W., Araki, Y., Use of shape-memory alloys in construction: A critical review, ICE Proceedings Civil Engineering, 169(2) (2016), 87–95.

Chou, C., C. Hsiao, Z. Chen, P. Chung, D. Pham, D., Seismic loading tests of full-scale two-story steel building frames with self-centering braces and buckling-restrained braces. Thin-Walled Structures, 140 (2019), 168-181.

Dan, M. B., Decision making based on benefit-costs analysis: Costs of preventive retrofit versus costs of repair after earthquake hazards. Sustainability (Switzerland), 10(5) (2018) doi:10.3390/su10051537 .

Dell'Aglio, G., R., Montuori, E. Nastri, V. Piluso, A critical review of plastic design approaches for failure mode control of steel moment resisting frames, Ingegneria Sismica, 34(4) (2017), 82–102.

Fraternali, F., Carpentieri, G., Amendola, A., Skelton, R.E., Nesterenko, V. F., Multiscale tunability of solitary wave dynamics in tensegrity metamaterials, Applied Physical Letters 105 (2014), 201903.

Fraternali, F., A. Amendola, G. Benzoni, Innovative seismic isolation devices based on lattice materials: A review, Ingegneria Sismica, 35(4) (2018), 93-113.

Fugazza, D., Shape-memory alloy device in earthquake engineering: Mechanical propreties, constitutive modelling and numerical simulations, Master's thesis, Rose School. Europeean School of Advanced Studies in Reduction of Seismic Risk, Pavia, Italy (2003).

Goyal, R., Perrera Hernandez, E.A., Skelton, R.E., Analytical study of tensegrity lattices for mass-efficient mechanical energy absorption, International Journal of Space Structures 0956059919845330 (2019).

Giugliano, M.T., Longo, A., Montuori, R., Piluso, V. Plastic design of CB-frames with reduced section solution for bracing members(2010) Journal of Constructional Steel Research, 66 (5), pp. 611-621.

Giugliano, M.T., Longo, A., Montuori, R., Piluso, V. Failure mode and drift control of MRF-CBF dual systems(2010) Open Construction and Building Technology Journal, 4, pp. 121-133.

HAZUS-MH, Multi-hazard loss estimation methodology: earthquake model, FEMA, http://www.fema.gov/hazus (2003).

Juan, S.H., J. M. M. Tur, Tensegrity frameworks: Static analysis review, Mechanism and Machine Theory 43 (7) (2008) 859 – 881.

Longo, A., Montuori, R., Piluso, V. Seismic reliability of chevron braced frames with innovative concept of bracing members (2009) Advanced Steel Construction, 5 (4), pp. 367-389.

Longo, A., Montuori, R., Piluso, V. Moment frames – concentrically braced frames dual systems: analysis of different design criteria (2016) Structure and Infrastructure Engineering, 12 (1), pp. 122-141.

Mathias, N., F. Ranaudo, M. Sarkisian, Mechanical amplification of relative movements in damped outriggers for wind and seismic response mitigation, International Journal of High-Rise Buildings 5 (1) (2016) 51–62.

Menna, C., Auricchio, F., Asprone, D. Applications of shape memory alloys in structural engineering. In: Concilio L, Lecce A, editors. Shape memory alloy engineering. Boston: Butterworth-Heinemann (2015), 369-403 [chapter 13].

Miller, D. J., L. A. Fahnestock, M. R. Eatherton, Development and experimental validation of a nickel-titanium shape memory alloy self-centering buckling-restrained brace, Engineering Structures 40 (2012) 288 – 298.

Montuori, R., E. Nastri, V. Piluso, Preliminary analysis on the influence of the link configuration on seismic performances of MRF-EBF dual systems designed by TPMC, Ingegneria Sismica, 33(3) (2016), 52–64

Montuori, R., E. Nastri, V. Piluso, Problems of modeling for the analysis of the seismic vulnerability of existing buildings. Ingegneria Sismica, 36(2) (2019), 53-85.

Montuori, R., R.E. Skelton, Globally stable tensegrity compressive structures for arbitrary complexity, Composite Structures, 179 (2017), 682–694.

Mouroux, P.,B. L. Brun, RISK-UE Project: An Advanced Approach to Earthquake Risk Scenarios With Application to Different European Towns, Springer Netherlands, Dordrecht, 2006, pp. 479–508.

Ohtori, Y., R. E. Christenson, J. B. F. Spencer, S. J. Dyke, Benchmark control problems for

seismically excited nonlinear buildings, Journal of Engineering Mechanics 130 (4) (2004) 366–385.

Piluso, V., Montuori, R., Nastri, E., Paciello, A. Seismic response of MRF-CBF dual systems equipped with low damage friction connections (2019) Journal of Constructional Steel Research, 154, pp. 263-277.

Rimoli, J.J., A reduced-order model for the dynamic and post-buckling behavior of tensegrity structures, Mechanics of Materials 116 (2018), 146–157.

SAC Steel Project https://www.sacsteel.org/.

SeismoStruct User Manual version 7.0 https://www.seismosoft.com/Public/EditorUpload/Documents/SeismoStruct_User_Manual_en.pdf.

Șigaher, A.N., Constantinouu, M.C., Scissor-jack-damper energy dissipation system, Earthquake Spectra, 19(1) (2003), 133–158.

Skelton, R.E., de Oliveira, M.C., Tensegrity Systems, Springer, Berlin, 2010.

Skelton, R.E., R. Montuori, V. Pecoraro, Globally stable minimal mass compressive tensegrity structures. Composite Structures, 141 (2016), 346-354.

Skelton, R., J. Helton, R. Adhikari, J. Pinaud, W. Chan, An introduction to the mechanics of tensegrity structures, in: Handbook of Mechanical Systems Design, CRC Press, 2002.

Steel Beams ASTM A36 https://www.mckinseysteel.com/pdf/WBeams.pdf .

Sultan, C., M. Corless, R. E. Skelton, Linear dynamics of tensegrity structures, Engineering Structures 24 (6) (2002) 671 – 685.

Yang, C. W., R. DesRoches, R. T. Leon, Design and analysis of braced frames with shape memory alloy and energy-absorbing hybrid devices, Engineering Structures 32 (2) (2010) 498 – 507.

ingegneria sismica
International Journal of Earthquake Engineering
Anno XXXVI – Num.3

RISPOSTA SISMICA DI CONTROVENTI TENSEGRITY A COMPORTAMENTO SUPERELASTICO

Filipe Santos[1], *Gianmario Benzoni*[2], *Fernando Fraternali*[3]

[1]CERIS and Department of Civil Engineering, Faculdade de Ciências e Tecnologia, Universidade Nova de Lisboa, Caparica, Portugal

[2]Department of Structural Engineering, University of California San Diego, CA, USA

[3]Department of Civil Engineering, University of Salerno, Fisciano (SA), Italy

SOMMARIO: *Questo articolo studia l'applicazione in campo antisismico di un sistema di confrovento superelastico con architettura tensegrity. La risposta di tipo metamateriale di un controvento a forma romboidale formato da 4 puntoni e due cavi in lega Nickel-Titanio a memoria di forma, consente di progettare un dispositivo di controllo passivo con massa ridotta ed elevate capacità di dissipazione energetica sotto eventi sismici. Il controvento proposto funziona come un amplificatore meccanico degli spostamenti longitudinali in direzione trasversale e consente di amplificare significativamente gli spostamenti relativi di piano del telaio al quale è collegato in direzione trasversale, favorendo la dissipazione di energia per effetto del comportamento superelastico dei cavi in Nickel-Titanio, in assenza di deformazuioni permanenti. Le elevate capacità di dissipazione di energia e di ricentramento del controvento tensegrity-SMA proposto sono dimostrate attraverso test sperimentali e la simulazione della risposta sismica sotto erremoti storici di una struttura campione. Il dismostrato, elevato potenziale ingegneristico di tale sistema di controvento nel ridurre il danneggiamento sismico dell'edificio servito apre la strada alla progettazione di nuovi dispositivi di dissipazione sismica dell'energia che combinino concetti tensegrity e di superelasticità.*

PAROLE CHIAVE*: Progettazione antisismica, Sistemi di controvento, Strutture tensegrity, Leghe a memoria di forma, Dissipazione di energia, Ricentramento*

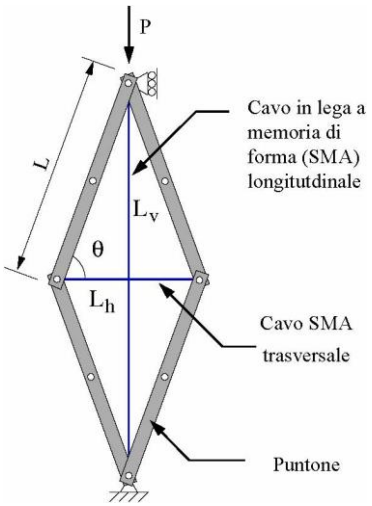

Sistema di controvento analizzato.

Corresponding author: Fernando Fraternali, Department of Civil Engineering, University of Salerno, Italy.
Email: f.fraternali@unisa.it